

See discussions, stats, and author profiles for this publication at: <https://www.researchgate.net/publication/249356366>

Effect of Fiber Orientation on Compressive Behavior of CFRP-confined Concrete Columns

Article in *Journal of Reinforced Plastics and Composites* · May 2010

DOI: 10.1177/0731684409102985

CITATIONS

5

READS

30

3 authors:



[Pedram Sadeghian](#)

Dalhousie University

28 PUBLICATIONS 78 CITATIONS

[SEE PROFILE](#)



[Alireza Rahai](#)

Amirkabir University of Technology

72 PUBLICATIONS 482 CITATIONS

[SEE PROFILE](#)



[Mohammad R. Ehsani](#)

The University of Arizona

75 PUBLICATIONS 2,811 CITATIONS

[SEE PROFILE](#)

Some of the authors of this publication are also working on these related projects:



Experimental and numerical assessment of the behavior of slender concrete columns reinforced with GFRP, and steel RC columns strengthened with longitudinal CFRP strips using bonded or near surface mounted (NSM) technique [View project](#)



Connections of Concrete-Filled FRP Tubes to Concrete Members [View project](#)

All content following this page was uploaded by [Pedram Sadeghian](#) on 03 April 2017.

The user has requested enhancement of the downloaded file. All in-text references [underlined in blue](#) are added to the original document and are linked to publications on ResearchGate, letting you access and read them immediately.

Effect of Fiber Orientation on Compressive Behavior of CFRP-confined Concrete Columns

Pedram Sadeghian ^{a,*}, Ali R. Rahai ^b, Mohammad R. Ehsani ^c

^a Department of Civil and Architectural Engineering, Islamic Azad University of Qazvin
Nokhbegan St., Daneshgah Blvd., Qazvin, Iran

^b Department of Civil and Environmental Engineering, Amirkabir University of Technology
No. 424, Hafez St., Enghelab Av., Tehran, Iran

^c Department of Civil Engineering and Engineering Mechanics, University of Arizona
Bldg. No. 72, Room 206, Tucson, AZ 85721, USA

* Corresponding author. Tel.: +98-912-200-2568; fax: +98-21-8879-6665

E-mail address: Sadeghian@qazviniau.ac.ir (P. Sadeghian)

Abstract:

This paper presents the results of experimental studies about concrete cylinders confined with high-strength carbon fiber reinforced polymer (CFRP) composites. Thirty small scale specimens (150×300 mm) were subjected to uniaxial compression up to failure and stress-strain behaviors were recorded. The various parameters such as wrap thickness and fiber orientation were considered. Different wrap thicknesses (1, 2, 3, and 4 layers), fiber orientation of 0°, 90°, ±45° and combinations of them were investigated. The results demonstrated significant enhancement in the compressive strength, stiffness, and ductility of the CFRP-wrapped concrete cylinders as compared to unconfined cases. An analytical model for ultimate stress and strain of confined concrete has been proposed.

Keywords: CFRP; Fiber orientation; Experiment; Ductility; Confinement; Strengthening; Concrete column.

Introduction

In recent years, the use of fiber reinforced polymers (FRP) as an externally wrapping have achieved considerable popularity for the strengthening and repair of concrete structures. The FRP composites have been used successfully for rehabilitation and strengthening of deficient reinforced concrete elements. The potential market for such applications is huge since the estimated annual cost of repairing bridges in the United States alone is 9.4 billion dollars [1].

One popular technique of FRP strengthening is the wrapping of reinforced concrete columns to increase their axial strength, shear strength, and seismic resistance. In this application, the FRP sheets are generally wrapped around the columns with fibers oriented mainly in the circumferential (hoop) direction. The fibers confine the concrete and increase the axial strength by creating a triaxial stress condition. The FRP wraps also increase the shear resistance of columns and prevent premature failures when columns are subjected to lateral loadings typical of those observed during earthquakes. [1]

Reinforced concrete columns need to be laterally confined in order to ensure large deformation under applied loads before failure and to provide an adequate bearing capacity. In the case of a seismic event, energy dissipation allowed by a well-confined concrete core can often save lives. On the contrary, a poorly confined concrete column behaves in a brittle manner leading to sudden and catastrophic failures. [2]

When the FRP-wrapped concrete is subjected to an axial compression loading, the concrete core expands laterally. This expansion is resisted by the FRP wrap, and therefore the concrete core is changed to a three dimensional compressive stress state. In this state, performance of the concrete core is significantly influenced by the confinement pressure [3]. Several parameters influence the confinement effectiveness of the FRP wrap, which include

concrete strength, wrap thickness or number of FRP layers, and wrap angle orientation [4].

Many investigations have been conducted into the behavior of FRP-wrapped concrete,

For a column subjected to a uniaxial compressive load, it is well established that fibers should be aligned along the hoop direction to confine the dilation of the concrete core. In practice, however, almost all the columns are subjected to an eccentric axial load, which can be resolved into a uniaxial compressive load and a bending moment. Because of this, almost all the columns should be treated as beam-columns. For beam-column, hoop direction is the optimal fiber orientation only for uniaxial compressive load; for a bending moment, fibers in the axial direction are more favorable. Therefore, fiber orientation is an important variable in the structural design of FRP-wrapped concrete columns. [5]

In the present paper, focuses are on applications of carbon FRP (CFRP) wraps with various fiber orientations and wrap thickness to increase the axial strength and ductility of unreinforced circular concrete columns.

Background

A number of studies have been conducted on different configurations for fiber orientations and various wrap thicknesses. Mirmiran and Shahawy [6] conducted experiments on axially loaded 152.5×305 mm concrete-filled FRP tubes made of unidirectional E-glass fibers at $\pm 15^\circ$ winding angle. Various jacket thicknesses of 6, 10, and 14 plies were examined, while winding angle was fixed. Their findings indicated that, as the jacket thickness increased, the strength and ductility increased as well. However, their study was concentrated on one winding angle configuration ($\pm 15^\circ$ winding angle) with no further discussion on this parameter.

Rochette and Labossiere [5] studied the influence of wrap thickness and cross section shape (circular, square, and rectangular) on the column strength. The wraps had 0° angle

orientation with respect to horizontal axis with the exception of one square column which was wrapped with the $\pm 15^\circ/0^\circ$ (angle-hoop) configuration. Their investigation on the fiber orientation was limited to one test and one angle-hoop configuration.

Pessiki et al. [7] performed experiments on small-scale square and circular plain concrete specimens under axial load. The FRP wrap were made of $0^\circ/\pm 45^\circ$ multidirectional GFRP, 0° unidirectional GFRP, and (0° unidirectional CFRP wraps. The compressive strength increased by 128% for small-scale circular specimens with one-ply $0^\circ/\pm 45^\circ$ GFRP jacket and 244% for circular specimens with two-ply 0° CFRP jackets. Additionally, as compared to unjacketed specimens, axial strains at peak stress have increased approximately seven times.

Parvin and Jamwal [8] studied the effect of wrap thickness and stacking sequence of plies with 0° and $\pm 45^\circ$ ply angles in the jacket through nonlinear finite element analysis. In another study, Parvin and Jamwal [9] investigated the performance of axially loaded, small-scale, and FRP-wrapped concrete columns with various wrap angle configurations, wrap thicknesses, and concrete strengths through nonlinear finite element analysis. Three different wrap thicknesses, wrap ply angle configurations of 0° , $\pm 15^\circ$, and $0^\circ/\pm 15^\circ/0^\circ$ with respect to the circumferential direction, were considered.

Li et al. [10] conducted an experimental study on 27 concrete cylinders wrapped with six fiber orientations. It is found that the strength, ductility, and failure mode of FRP wrapped concrete cylinders depend on the fiber orientation and wrap thickness. Fibers oriented at a certain angle in between the hoop direction and axial direction may result in strength lower than fibers along hoop or axial direction.

According to previous researches on the subject; there are a number of issues that need to be addressed: (a) how is stress-strain behavior of concrete cylinders confined by CFRP composites? The answer is important in order to refine the existing design-oriented confinement models, (b) what are effects of fiber orientations and wrap thicknesses on

strength and ductility of concrete cylinders confined with CFRP composites? , (d) how is mode of failure at $\pm 45^\circ$ wrap angle and what are the effects of $\pm 45^\circ$ wrap angle on shear cracks?, and (d) How do dilation characteristics of confined concrete perform with various wrap angle configurations?

The present study is an experimental investigation on concrete cylinders confined with CFRP composites under axial loading. For response to the above questions, a number of unreinforced concrete cylinders were prepared and wrapped with CFRP composites with different configurations of fiber orientations and various wrap thicknesses. Then an analytical modeling was performed on stress-strain behavior of CFRP-wrapped circular concrete cylinders. The experimental and analytical studies are discussed in the following sections.

Experimental Program

Specimen Layout

A total of 23 CFRP-wrapped and 7 unconfined control concrete cylinders with a diameter of 150 mm and a height of 300 mm were prepared and tested under uniaxial compression loading. The main experimental parameters were included wrap thickness and fiber orientation. Four different wrap thicknesses 0.9, 1.8, 2.7, and 3.6 mm (1, 2, 3, and 4 layers) and four fiber orientation of 0° , 90° , $+45^\circ$, and -45° with respect to the hoop direction were investigated. The test program and specimen properties are summarized in Table 1, where L is for when the fibers are aligned with the longitudinal axis of the cylinder (90°) and T corresponds to placing the fibers such that they are in the hoop direction or transverse to the longitudinal axis of the cylinder (0°). In addition, D and D' are for when fibers are aligned with the diagonal direction ($+45^\circ$) and the inversed diagonal direction ($+135^\circ$ which is the same as -45°). The fiber orientations are shown in Fig. 1.

Material Properties

Target compression strength of plain concrete at 28 days was 30 MPa. However, actual compression strength of plain specimens at the test day were measured 35 MPa up to 45 MPa. The quantities of components were used in the concrete mix are shown in Table 2. A unidirectional carbon fiber sheet was used to prepare the CFRP wrap. Table 3 provides the properties of carbon fibers as supplied by the manufacturer. Table 4 shows the properties of cured resin as supplied by the manufacturer. Mechanical properties of CFRP wraps have been recorded through tension tests on CFRP coupons by Sadeghian et al. [11]. The average test results in fiber and matrix direction are shown in Table 5.

Specimen Preparation

The concrete was produced with a similar mixture design before casting in standard cylindrical formworks. After curing in humid room for 28 days, the surface of specimens were cleaned and prepared for wrapping. In order to prevent anchorage rupture in CFRP-wrap, a lap splice equal to 75 mm was used in fiber direction. The carbon fiber sheet was cut and impregnated with epoxy resin by the hand lay-up technique. The epoxy resin consisted of two components, the main resin and the hardener. The mixing ratio of the components by weight was 100:15 and they were mixed for three minutes. The carbon fibers were configured in predefined orientations as shown in Table 1, and then were impregnated with the epoxy resin. Epoxy resin should be cured in laboratory temperature for a minimum of seven days.

Test Setup and Loading

In order to perform uniaxial compression testing on specimens, a hydraulic testing machine was used in the Amirkabir University of Technology (Strength of Material Laboratory). Bottom jaw of the machine is adjustable in the vertical direction and it is

attached to an actuator, while the top jaw is fixed. The specimens were tested using a 3,000 KN capacity compression machine and the data were monitored using an automatic data acquisition system. The tests were continued up to failure under a monotonically increasing concentric load in a displacement control mode. The force and displacement data were obtained by data collecting system of the machine during the test and were stored for future reduction and analysis.

Experimental Results and Discussions

Overall Behavior

The performance of the cylinders under axial load was consistent. At the early stages of loading of the confined specimens, the noise related to the micro cracking of concrete core was evident, indicating the start of stress transfer from the dilated concrete to the CFRP wrap. Prior to the failure, cracking noises were frequently heard. The failure was gradual, ending with a sudden and explosive noise.

The failure of the wrap initiated away from the overlap region at mid-height of the specimen and progressed to the top and bottom of the specimen. The sudden and explosive nature of the failure indicates the release of extraordinary amount of energy as a result of the uniform confining stress provided by the wrap. Inspection of the broken samples showed good contact between the wrap and the concrete indicating that no debonding took place at any stage throughout the loading process, as is clearly demonstrated by the wrapped specimens in Fig. 2.

Plain Specimens

The axial stress-strain curves for the plain specimens are presented in Fig. 3. This figure shows that the unconfined concrete strength varies between 35 and 45 MPa and the

corresponding strain of the unconfined concrete strength varies between strain of 0.2 and 0.25 percent. The average unconfined concrete strength of 40 MPa and corresponding strain of 0.22 percent was calculated.

Transverse Orientation

Typical axial stress-strain curve of wrapped specimen with one layer of transverse orientation (T) along by the average axial stress-strain curve of plain specimens are presented in Fig. 4. This figure shows that the confined concrete strength is increased from about 39 MPa to 79MPa and ultimate strain of confined concrete is increased from about 0.22% to 0.62%.

Axial stress-strain behavior of wrapped specimens with 1, 2, 3, and 4 CFRP wraps with transverse orientations (T, TT, TTT, and TTTT) are shown in Fig. 5. This figure shows that the confined concrete strengths with two layers are 91.9 and 96.4 MPa; the ultimate strains are 0.96% and 0.86%, the confined concrete strengths with three layers are 124.9 and 125.7 MPa; the ultimate strains are 1.61% and 1.32%, and finally the confined concrete strength with four layers is 143.3 MPa; with ultimate strain of 1.76%. For every specimen, a stress-strain behavior with the three zones similar to the first specimen can be defined.

So the stress-strain behavior of the confined specimen can be considered in three zones. In the first zone, the behavior of confined concrete is mostly linear and similar to unconfined (plain) concrete. In second zone, lateral strain increases and the wrap is activated. So proportionate with the lateral strain, the wrap is stretched and a tension stress is produced in hoop direction. This action produces a confinement stress on concrete core. In third zone, because of large lateral strain, the wrap becomes fully activated and the confinement stress increases in proportion to the hoop stiffness of wrap. The first and third zones are approximately linear and the second zone as a transition zone is nonlinear.

Longitudinal Orientation

Axial stress-strain curves for wrapped specimens with 1, 2, and 3 layers of pure longitudinal orientations (L, LL, and LLL) along by the plain specimen are presented in Fig. 6. This figure shows that the pure longitudinal orientations have not significantly enhanced the strength and ductility of the specimens under uniaxial compression. The effect of pure longitudinal orientation can be neglected, because the fibers have little lateral support and buckle under uniaxial compression.

Fig. 7 shows results of wrapped specimens with combination of transverse and longitudinal orientations (two specimens with LT, two specimens with TL, and one specimen with LLT). It is shown that the behavior of specimens with combined fiber orientations are very similar to those with fibers placed in the transverse orientation. The strength, ductility, and stiffness of wrapped specimens with combination of transverse and longitudinal orientations are controlled primarily by the contribution of the fibers in the transverse orientation.

Angle Orientation

The behaviors of wrapped specimens with angle orientations DD' and DD'DD' are presented in Fig. 8. This figure shows that the angle of orientation of fibers has a substantial influence on the stiffness of the specimens. The stress-strain curve of wrapped specimens with fibers in the transverse orientation is a bilinear behavior with a positive slope; however, when the angle of fibers is changed to $\pm 45^\circ$, the behavior is accompanied by a larger flat region prior to failure. This behavior can be very useful in cyclic loading and hysteretic damping against seismic loading. In the DD'DD' angle orientation with four layers, ultimate stress and strain are about 74.2 MPa and 2.22% , respectively, while yielding range is about 1.5%. In the DD' angle orientation with two layers, ultimate stress and strain are about 60.0

MPa and 0.74% , respectively, while yielding range with a premature failure is about 0.2%.

So the angle orientations have a significant influence on enhancement of ductility and energy dissipation.

Fig. 9 shows the stress-strain behavior of wrapped specimens with combination of angle and transverse orientations. Two specimens with TDD' and DD'T orientations along by DD' and TTT orientations are compared. It is shown that the overall behavior of TDD' and DD'T orientations is similar to pure transverse orientations, not to pure angle orientations. These two specimens have a bilinear behavior with a lower second slope, and the failure is controlled by the transverse layer. The DD'T orientation on the average has a lower second slope than the TDD' orientations, because due to shear lag, the inner layers are activated sooner than the outer layers.

The combination of angle and transverse orientation is studied in Fig. 10. It is shown that LDD' orientations (with two specimens) have an elastic-perfect plastic similar to DD' orientation, so the longitudinal layers have not considerable effects on the stress-strain behavior. The ultimate strains of these specimens are about 1.35%. In comparison of DD' with these specimens, it can be concluded that DD' orientation has a premature failure, so its ultimate strains is predicted equal to about 1.35%.

Fig. 11 shows results of combination orientations in specimens of TDD'T, DD'TT, and LTDD'. The stress-strain curves of these specimens are bilinear and are controlled by behavior of hoop layers because of higher stiffness. When the hoop layers reach to ultimate strength and are broken, their hoop forces are transferred on the angle layers as impulsive forces. The angle layers can't resist the magnified forces, so the wrap suddenly is broken. As a result, the combination of hoop and angle orientation is not useful in these cases and the angle layers can't produce plastic deformations.

Analytical Modeling

Mechanism of confinement

By wrapping the concrete with an external continuous CFRP wrap, the fibers in the hoop direction resist the transverse expansion of the concrete providing a confining pressure. At low levels of longitudinal stress; however, the transverse strains are so low that the FRP jacket induces little confinement, if any. At higher longitudinal stress levels, the dramatic increase in transverse tensile strains activates the CFRP wrap and the confining pressure becomes more significant. The general confining pressure induces a triaxial state of stress in the concrete. It is well understood that concrete under triaxial compressive stress exhibits superior behavior, in both strength and ductility, as compared to concrete in uniaxial compression [12]. Fig. 12 shows the mechanism of confinement on a circular section with CFRP wrap.

Proposed Model

In a circular concrete column, the confining pressure is constant around the circumference, provided small variations due to factors such as the inhomogeneity of concrete are ignored. When the CFRP wrap ruptures, this confining pressure reaches its maximum value given by

$$f_r = \frac{2tf_j}{D}, \quad (1)$$

where f_r is confining pressure, t is wrap thickness, f_j is ultimate tensile strength of wrap in hoop direction, and D is diameter of concrete core. In this paper two global forms for ultimate stress and strain of CFRP-confined concrete are used by

$$\frac{f'_{cc}}{f'_{co}} = 1 + k \left(\frac{f_r}{f'_{co}} \right)^n, \quad (2)$$

$$v_{cc} = v_{co} + \left\{ \left(\frac{f_r}{f'_{co}} \right)^m \right\}, \quad (3)$$

where f'_{cc} is confined concrete strength, f'_{co} is plain concrete strength, v_{cc} is confined concrete strain at f'_{cc} , v_{co} plain concrete strain at f'_{co} (Fig. 12), k , n , $\}$, and m are constant factors. The constant factor can be calculated by a regression analysis. For this analysis the errors between analytical model and experimental data are calculated by

$$e_1 = 1 + k \left(\frac{f_r}{f'_{co}} \right)^n - \left(\frac{f'_{cc}}{f'_{co}} \right)_{ex}, \quad (4)$$

$$e_2 = v_{co} + \left\{ \left(\frac{f_r}{f'_{co}} \right)^m \right\} - (v_{cc})_{ex}, \quad (5)$$

where e_1 is the error of stress model, e_2 is the error of strain model, $\left(\frac{f'_{cc}}{f'_{co}} \right)_{ex}$ and $(v_{cc})_{ex}$ are

experimental data. Error functions (f_1, f_2) can be evaluated by SRSS (square root of sum of squares) methods by

$$f_1 = \sqrt{\sum e_1^2} = \sqrt{\sum \left(1 + k \left(\frac{f_r}{f'_{co}} \right)^n - \left(\frac{f'_{cc}}{f'_{co}} \right)_{ex} \right)^2}, \quad (6)$$

$$f_2 = \sqrt{\sum e_2^2} = \sqrt{\sum \left(v_{co} + \left\{ \left(\frac{f_r}{f'_{co}} \right)^m \right\} - (v_{cc})_{ex} \right)^2}, \quad (7)$$

The constant factors can be calculated by derivative of the error functions as defined below:

$$\frac{\partial f}{\partial k} = 0 \rightarrow \sum \left[\left(\frac{f_r}{f'_{co}} \right)^n \left(1 + k \left(\frac{f_r}{f'_{co}} \right)^n - \left(\frac{f'_{cc}}{f'_{co}} \right)_{ex} \right) \right] = 0, \quad (8)$$

$$\frac{\partial f}{\partial n} = 0 \rightarrow \sum \left[\left(\ln \frac{f_r}{f'_{co}} \right) \left(\frac{f_r}{f'_{co}} \right)^n \left(1 + k \left(\frac{f_r}{f'_{co}} \right)^n - \left(\frac{f'_{cc}}{f'_{co}} \right)_{ex} \right) \right] = 0, \quad (9)$$

$$\frac{\partial f}{\partial \beta} = 0 \rightarrow \sum \left[\left(\frac{f_r}{f'_{co}} \right)^m \left(v_{co} + \beta \right) \left(\frac{f_r}{f'_{co}} \right)^m - (v_{cc})_{ex} \right] = 0, \quad (10)$$

$$\frac{\partial f}{\partial n} = 0 \rightarrow \sum \left[\left(Ln \frac{f_r}{f'_{co}} \right) \left(\frac{f_r}{f'_{co}} \right)^m \left(v_{co} + \beta \right) \left(\frac{f_r}{f'_{co}} \right)^m - (v_{cc})_{ex} \right] = 0, \quad (11)$$

The above non linear equations have been expanded by MathCAD program and solved for the measured experimental data. This results in the proposed models that are presented in the following equations. Fig. 13 shows the comparison between experimental data and proposed model.

$$\frac{f'_{cc}}{f'_{co}} = 1 + 5.18 \left(\frac{f_r}{f'_{co}} \right)^{0.7}, \quad (12)$$

$$v_{cc} = v_{co} + 0.039 \left(\frac{f_r}{f'_{co}} \right)^{0.92}, \quad (13)$$

Conclusion

In an attempt to explain the behavior of concrete cylinders confined with high-strength carbon fiber reinforced polymer (CFRP) composites, thirty small scale specimens (150×300 mm) were subjected to uniaxial compression up to failure and stress-strain behaviors were recorded. Various parameters such as wrap thickness and fiber orientation were considered. Different wrap thicknesses (1, 2, 3, and 4 layers), fiber orientation of 0°, 90°, ±45° and combinations of them were investigated.

The enhancement of strength and ductility of CFRP confined concrete is significant. The observed stress-strain response of CFRP confined concrete can be divided in three distinct zones. The first zone is approximately linear and the second zone is nonlinear as a transition zone. The third zone depends on the wrap behavior. If the wrap has a linear behavior, slope of the third zone will be constant. If the wrap has a nonlinear behavior, the

third zone will have a decreasing slope. The specimens wrapped with hoop orientation have a bilinear behavior with a nonlinear transition zone. When the angle of fibers is changed to $\pm 45^\circ$, the behavior is accompanied by a larger flat region as a plastic deformation prior to failure. This behavior can be very useful in cyclic loading and hysteretic damping against seismic loading. The combination of hoop and angle orientation is not useful and the angle layers can't produce plastic deformations. At the end, an analytical model for ultimate stress and strain of confined concrete has been proposed.

Acknowledgement

The authors acknowledge the financial assistances of the Amirkabir University of Technology (Tehran Polytechnic) through, which enabled conducting this research. The technical assistance of Dr. A. Alizadeh of the Amirkabir University of Technology is appreciated.

References

- [1] Green MF, Bisby LA, Fam AZ, Kodur VKR. FRP confined concrete columns: Behaviour under extreme conditions. *Cement and Concrete Composites* 2006; **28** : 928-937.
- [2] [Kumutha R, Vaidyanathan R, Palanichamy MS. Behaviour of reinforced concrete rectangular columns strengthened using GFRP. *Cement and Concrete Composites* 2007; **29** :609-615.](#)
- [3] [Parvin A, Jamwal AS. Effects of wrap thickness and ply configuration on composite-confined concrete cylinders. *Composite Structures* 2005; **67** : 437-442.](#)
- [4] [Sadeghian P, Rahai AR, Ehsani MR. Numerical modeling of concrete cylinders confined with CFRP composites. *Journal of Reinforced Plastics and Composites* 2007; \(in press\).](#)

- [5] [Rochette P, Labossiere P. Axial testing of rectangular column models confined with composites. *Journal of Composites for Construction* 2000; **4** : 129-136.](#)
- [6] [Mirmiran A, Shahawy M. Behavior of concrete columns confined by fiber composites. *Journal of Structural Engineering* 1997; **123** : 583-590.](#)
- [7] [Pessiki S, Harries K, Kestner JT, Sause R, Ricles J.M. Axial behavior of reinforced concrete columns confined with FRP jackets. *Journal of Composites for Construction* 2001; **5** : 237-245.](#)
- [8] [Parvin A, Jamwal AS. Effects of wrap thickness and ply configuration on composite-confined concrete cylinders. *Composite Structures* 2005; **67** : 437-442.](#)
- [9] [Parvin A, Jamwal AS. Performance of externally FRP reinforced columns for changes in angle and thickness of the wrap and concrete strength. *Composite Structures* 2006; **73** : 451-457.](#)
- [10] [Li G, Maricherla D, Singh K, Pang S, John M. Effect of fiber orientation on the structural behavior of FRP wrapped concrete cylinders. *Composite Structures* 2006; **74** : 475-483.](#)
- [11] [Sadeghian P, Rahai AR, Ehsani MR. Fiber orientation effects on tensile properties of CFRP composites. *Journal of Reinforced Plastics and Composites* 2008; \(in press\).](#)
- [12] [Youssef MN, Feng MQ, Mosallam AS. Stress-strain model for concrete confined by FRP composites. *Composites: Part B-Engineering* 2007; **38** : 614-628.](#)

Table 1. Test program and specimen properties

| Specimen | Number of layers | Fiber orientation | Number of specimen |
|----------|------------------|-------------------|--------------------|
| P | - | Plain | 7 |
| T | 1 | 0° | 1 |
| TT | 2 | 0°/0° | 2 |
| TTT | 3 | 0°/0°/0° | 2 |
| TTTT | 4 | 0°/0°/0°/0° | 1 |
| L | 1 | 90° | 1 |
| LL | 2 | 90°/90° | 1 |
| LLL | 3 | 90°/90°/90° | 1 |
| TL | 2 | 0°/90° | 2 |
| LT | 2 | 90°/0° | 2 |
| LLT | 3 | 90°/90°/0° | 1 |
| DD' | 2 | ±45° | 1 |
| DD'DD' | 4 | ±45°/±45° | 1 |
| DD'T | 3 | ±45°/0° | 2 |
| TDD' | 3 | 0°/±45° | 1 |
| LDD' | 3 | 90°/±45° | 1 |
| DD'TT | 4 | ±45°/0°/0° | 1 |
| TDDT | 4 | 0°/±45°/0° | 1 |
| LTDD' | 4 | 90°/0°/±45° | 1 |

Table 2. Concrete mix design

| Component | Quantity (kg/m ³) |
|-----------|-------------------------------|
| Cement | 378 |
| Water | 193 |
| Sand | 640 |
| Gravel | 1133 |
| W/C | 0.51 |

Table 3. Properties ^a of unidirectional carbon fiber sheets

| Fibers | Ultimate tensile strength (MPa) | Elastic modulus (GPa) | Ultimate strain (%) | Nominal thickness (mm/ply) | Areal weight (g/m ²) |
|--------|---------------------------------|-----------------------|---------------------|----------------------------|----------------------------------|
| Carbon | 3860 | 242 | 1.6 | 0.25 | 332 |

^aReported by the manufacturer.

Table 4. Properties ^a of cured epoxy resin and hardener

| Material | Tension | | Compression | | Shear |
|----------|-------------------------|-----------------------|-------------------------|-----------------------|-------------------------|
| | Ultimate strength (MPa) | Elastic modulus (MPa) | Ultimate strength (MPa) | Elastic modulus (MPa) | Ultimate strength (MPa) |
| Epoxy | 76.1 | 2789 | 97.4 | 937 | 54.8 |

^a Reported by the manufacturer.

Table 5. Mechanical properties of CFRP composites [11]

| Fiber orientation | Ultimate strength (MPa) | Initial modulus (MPa) |
|-------------------|-------------------------|-----------------------|
| Fiber direction | 303 | 41000 |
| Matrix direction | 29 | 2400 |

Table 6. Experimental data for fiber orientation in transverse direction

| Specimen | Fiber orientation | f'_{cc} (MPa) | v_{cc} (%) | f_r (MPa) | $\frac{f_r}{f'_{co}}$ | $\frac{f'_{cc}}{f'_{co}}$ |
|----------|-------------------|-----------------|--------------|-------------|-----------------------|---------------------------|
| T | 0 | 79 | 0.62 | 3.6 | 0.09 | 1.98 |
| TT | 0/0 | 91.9 | 0.96 | 7.2 | 0.18 | 2.30 |
| TT | 0/0 | 96.4 | 0.86 | 7.2 | 0.18 | 2.41 |
| TTT | 0/0/0 | 124.9 | 1.61 | 10.8 | 0.27 | 3.12 |
| TTT | 0/0/0 | 125.7 | 1.32 | 10.8 | 0.27 | 3.14 |
| TTTT | 0/0/0/0 | 143.3 | 1.76 | 14.4 | 0.36 | 3.58 |
| LT | 90/0 | 83.2 | 0.55 | 3.6 | 0.09 | 2.08 |
| LT | 90/0 | 78.2 | 0.72 | 3.6 | 0.09 | 1.955 |
| TL | 0/90 | 78.8 | 0.67 | 3.6 | 0.09 | 1.97 |
| TL | 0/90 | 77.2 | 0.79 | 3.6 | 0.09 | 1.93 |
| LLT | 90/90/0 | 84.9 | 0.74 | 3.6 | 0.09 | 2.12 |

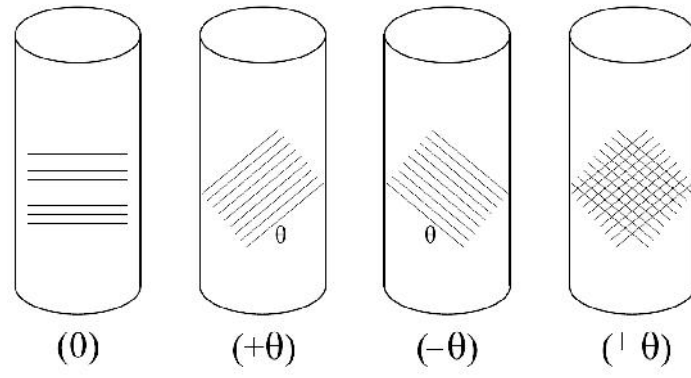


Fig. 1. Fiber orientation in CFRP-wrapped cylinders [4]



Fig. 2. Specimens at failure

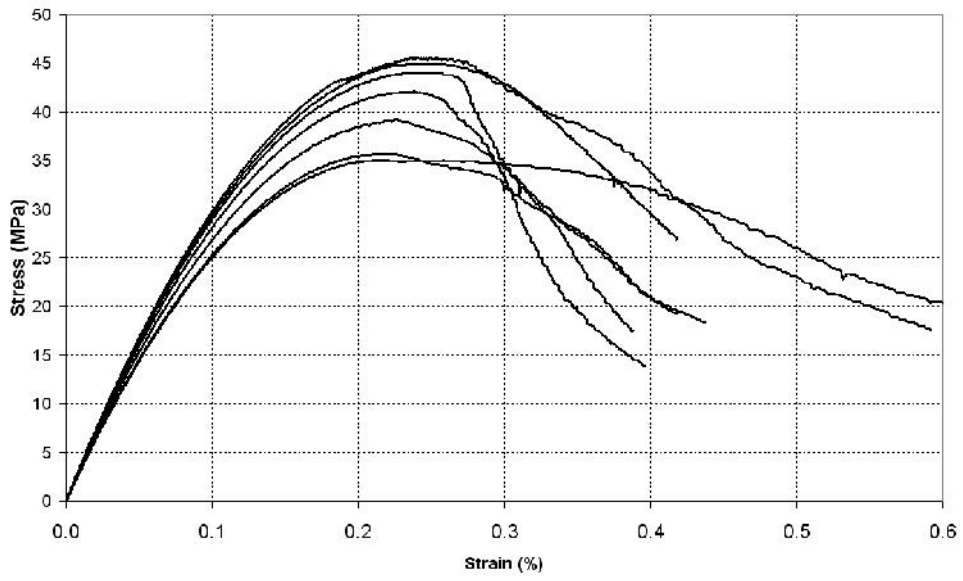


Fig. 3. Stress-strain behavior of plain specimens

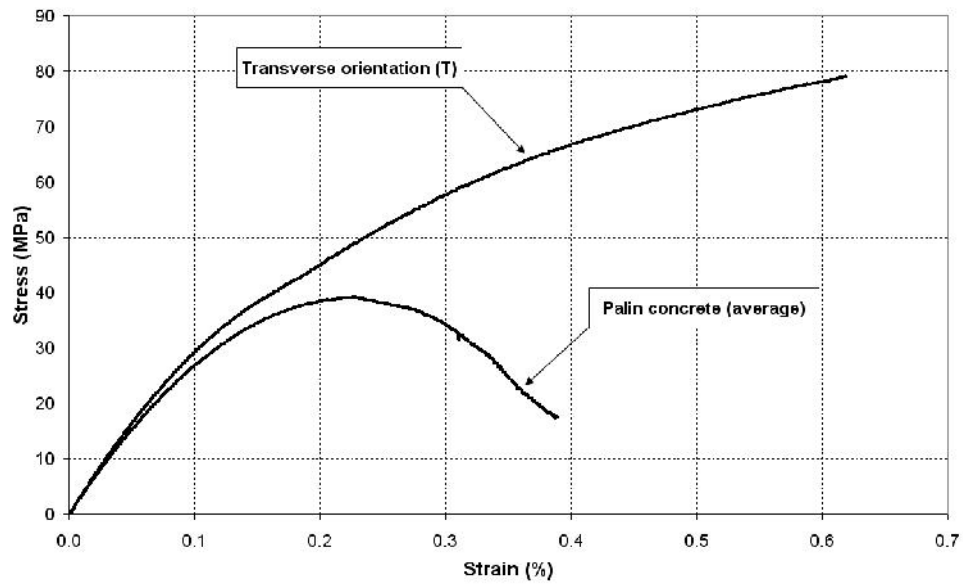


Fig. 4. Behavior of one layer wrapped specimen in hoop direction

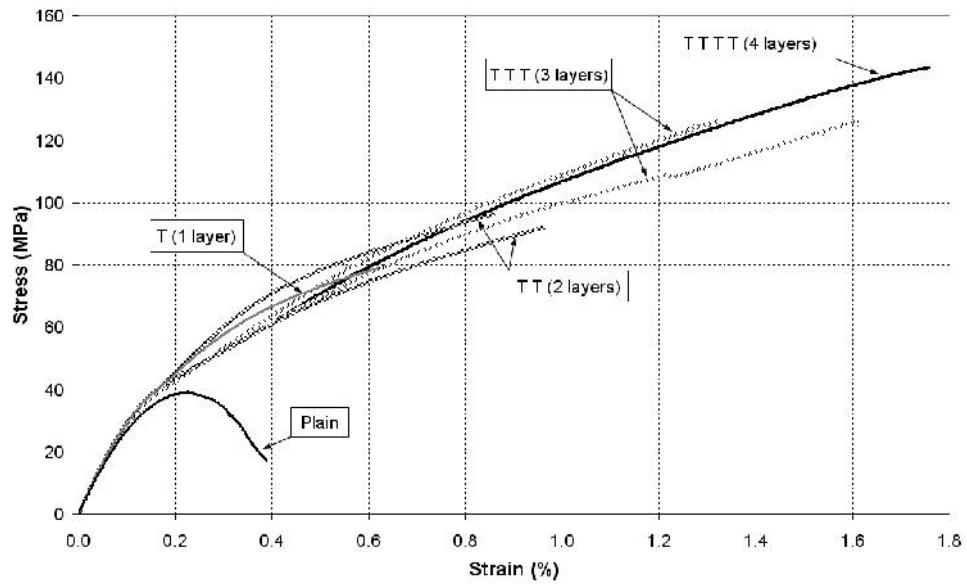


Fig. 5. Behavior of wrapped specimens with hoop orientations

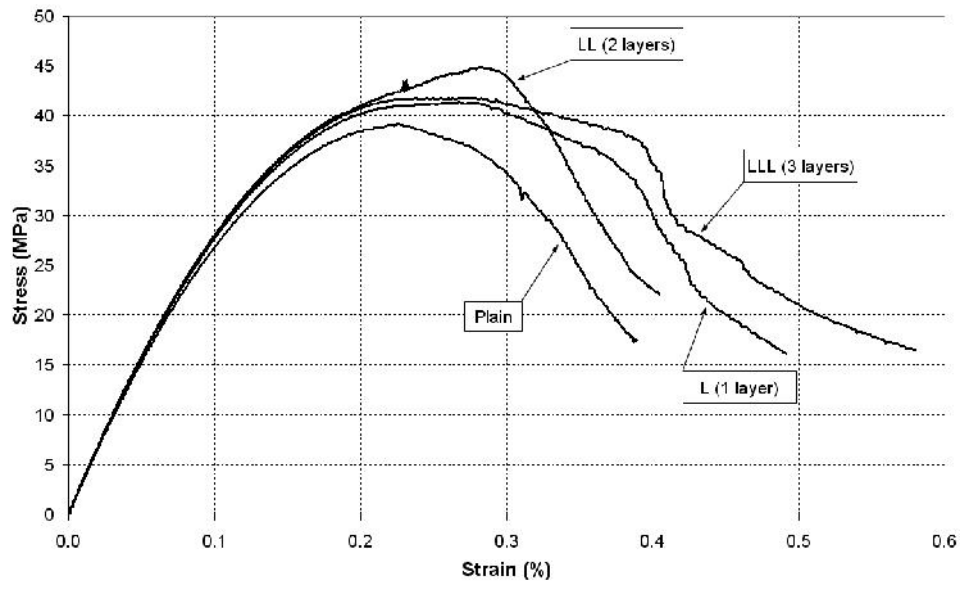


Fig. 6. Behavior of specimens with longitudinal orientations

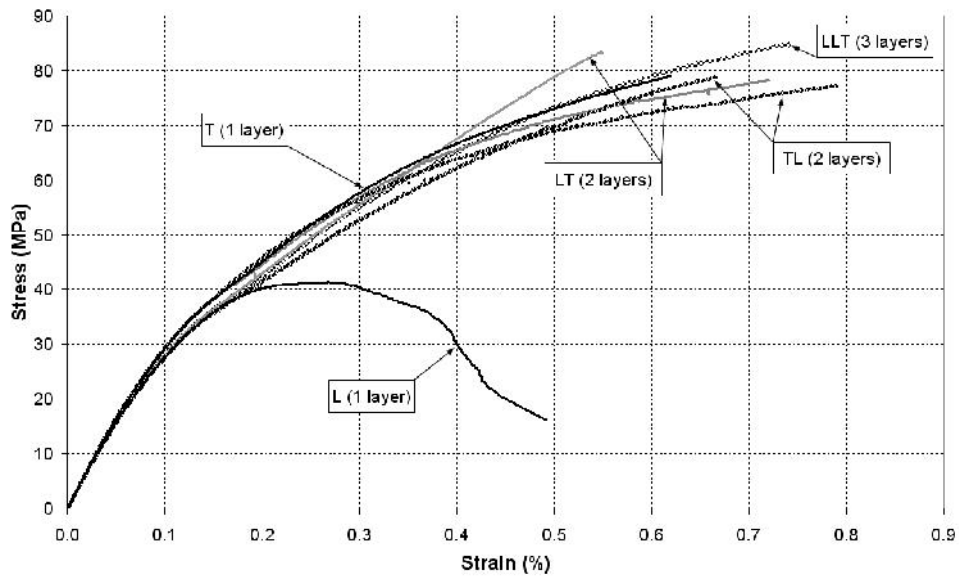


Fig. 7. Combination of transverse and longitudinal orientations

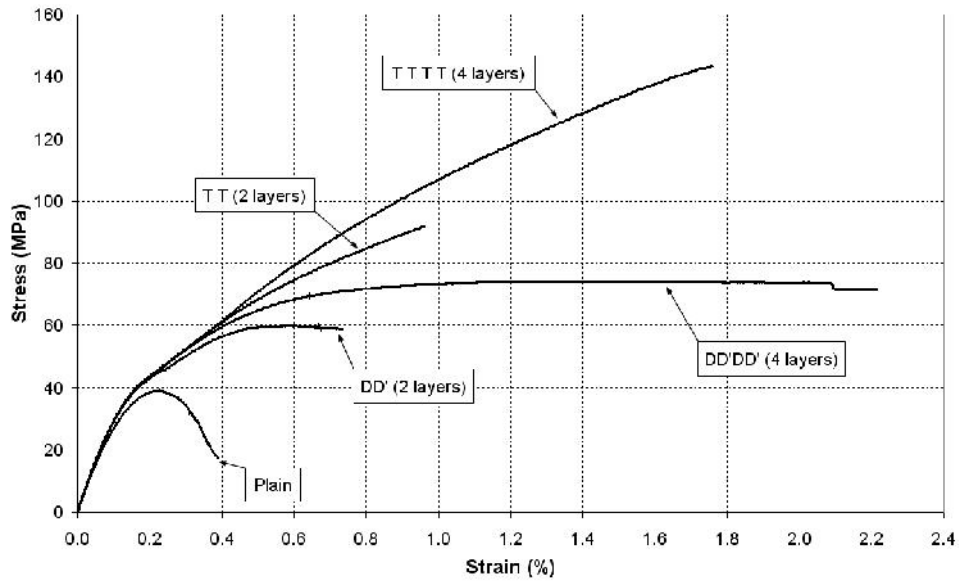


Fig. 8. Behavior of wrapped specimens with angle orientation

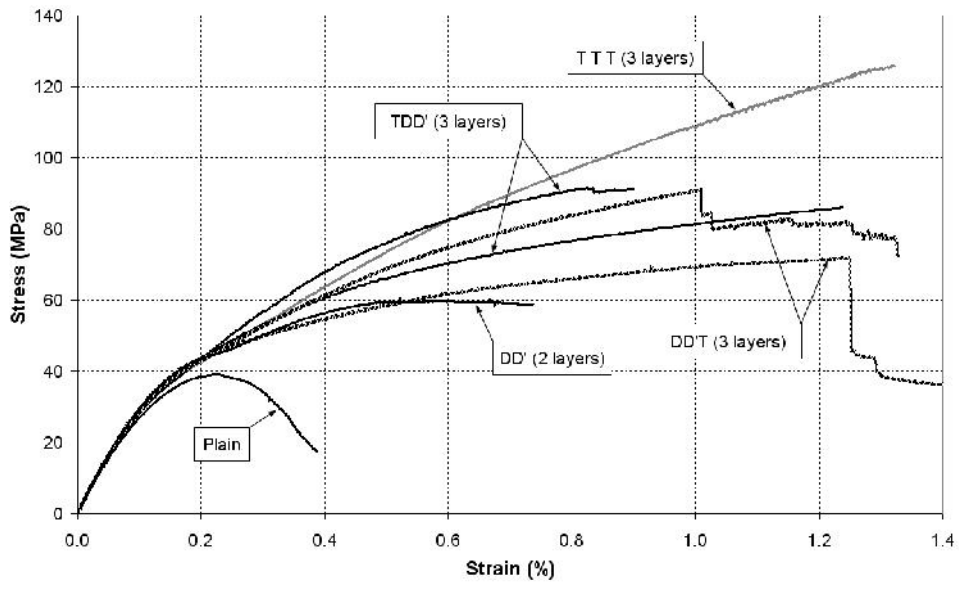


Fig. 9. Combination of angle and transverse orientation

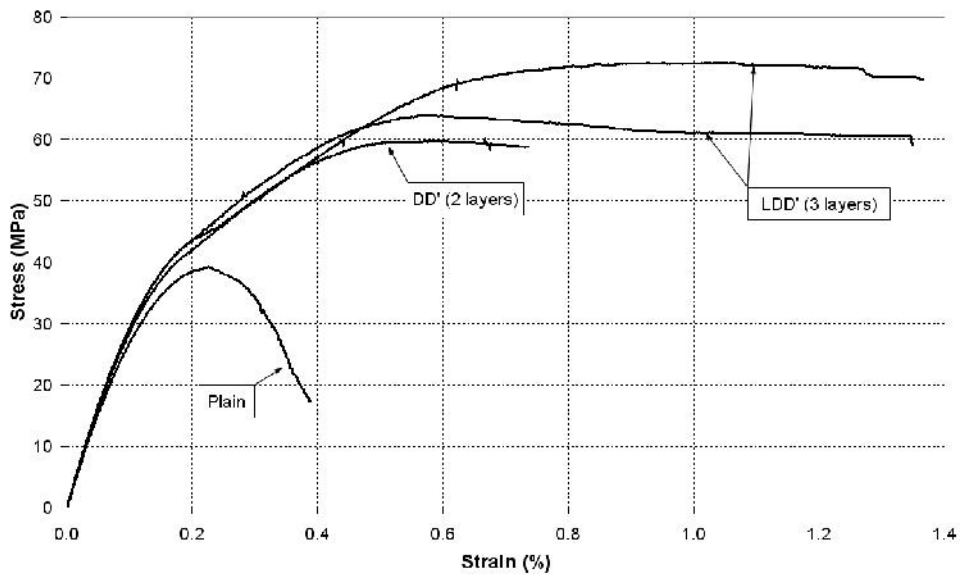


Fig. 10. Combination of angle and longitudinal orientation

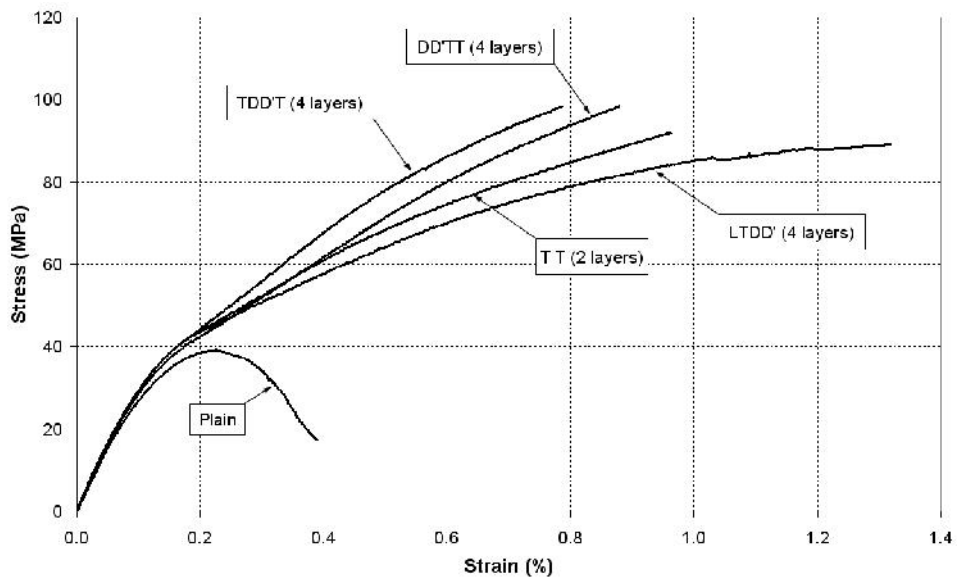


Fig. 11. Specimens with combination orientation

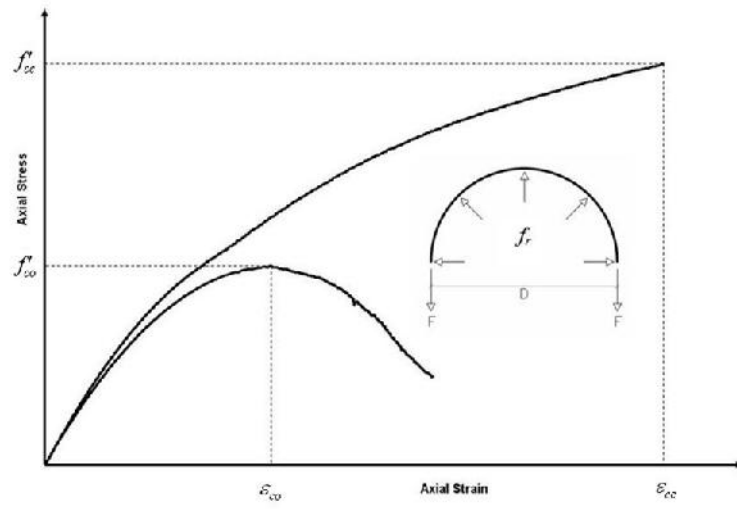


Fig. 12. Mechanism of confinement with CFRP wrap

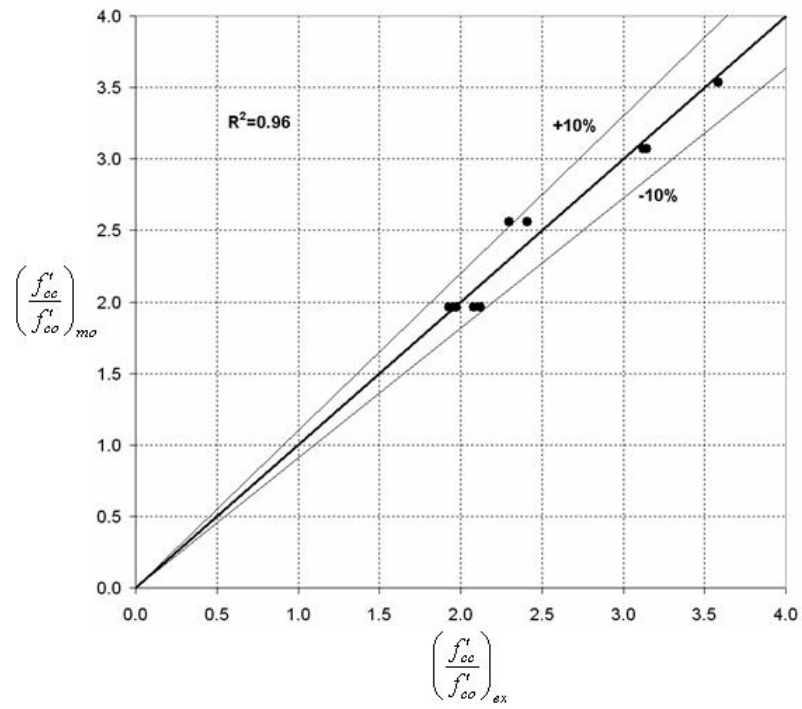


Fig. 13. Performance of proposed model for ultimate stress